4. Bed Evolution

4.1 Time evolution of scouring

The data acquired during the mobile-bed run have been analyzed in order to study the time evolution of bed topography. As observed in chapter 3, this run was performed for a time T = 480 min, at which the "equilibrium" configuration was reached. In Figure 4.1 is reported a definition sketch of the geometric parameters considered in the analysis of the scour hole obtained at the end of this run: the length, L_t, of scour hole, the maximum scour depth, Z_{min}, the longitudinal distance of the maximum scour from the rigid bed, L_{max}, and the total length of the scour phenomenon L_{tot}.

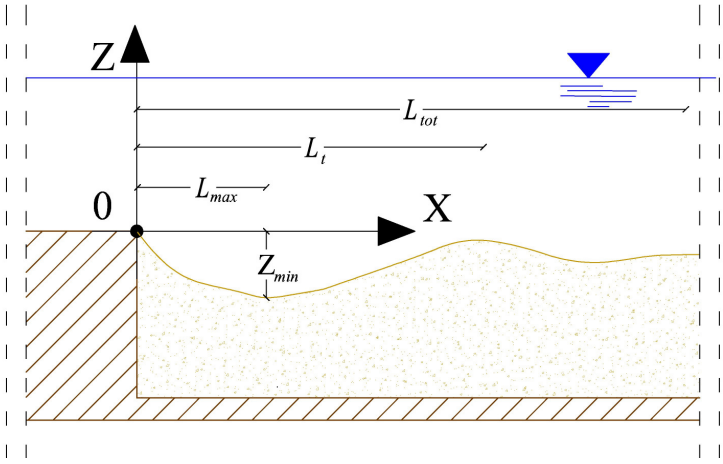

Figure 4.1 - Definition sketch of the geometric parameters.

During the mobile-bed run the bed elevation was measured in 92 cross sections (see Figure 3.7) with a time step of about 20-30 minutes. Thus, for each section, 25 profiles were measured. In order to analyze the evolution of the bed surface until the reaching of the equilibrium configuration, the instantaneous digital elevation model (DEM) has been determined for the considered time steps. Each instantaneous DEM has been obtained by interpolating the bed level data through the Kriging method by using the commercial code

SURFER (linear semi-variogram model with grid line geometry of ΔX = 5cm – ΔY = 1cm). The Kriging interpolation is a geostatistical technique that belongs to the family of linear least squares estimation algorithms. This technique interpolates the bed elevation at an unobserved location from observations at nearby locations. The analysis of the instantaneous DEM has allowed the verification of the evolution of the geometrical characteristics of the scour hole. In Figure 4.2 the DEM of the bed surface at the end of the mobile-bed run (channel reach 3 m long) and a zoomed view of the scour hole (channel reach 50cm long) are reported.

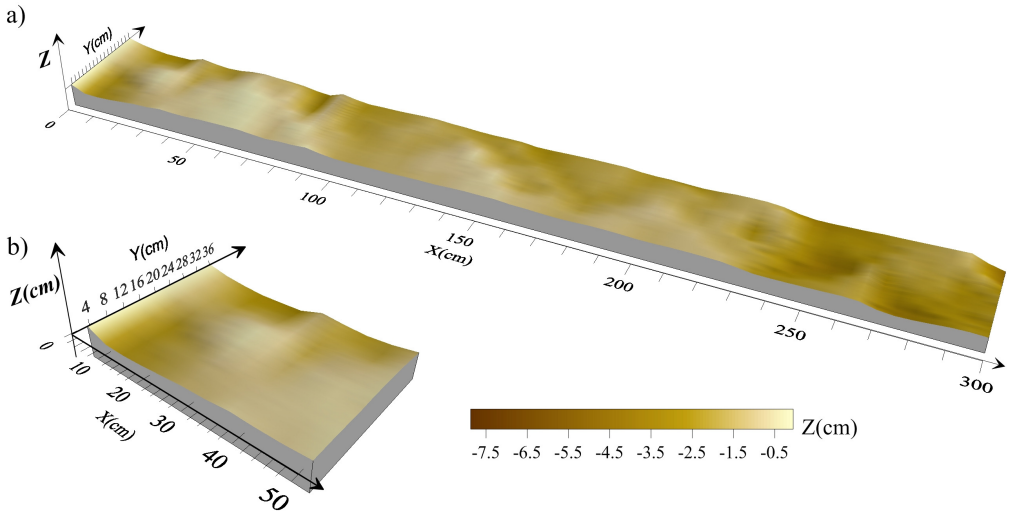

Figure 4.2 - DEM at the end of mobile-bed run: a) channel reach 3m long; b) zoomed view 50 cm long.

The DEM of the bed surface highlights that the scour hole develops along a channel reach 30 cm long; then a deposit front develops for a further length of 20 cm. Thus the scour phenomenon occurs along a channel reach of a total length L_{tot} of about 50 cm. Thus, in order to study the temporal evolution of the scour hole, only the sections in the range X0÷X50 will be analyzed in the following. Furthermore Figure 4.2 highlights that

two scour holes form almost symmetrically with respect to the channel axis. The contour map of this considered channel reach is reported in Figure 4.3. From the map of Figure 4.3 these two scour holes are clearly distinguishable.

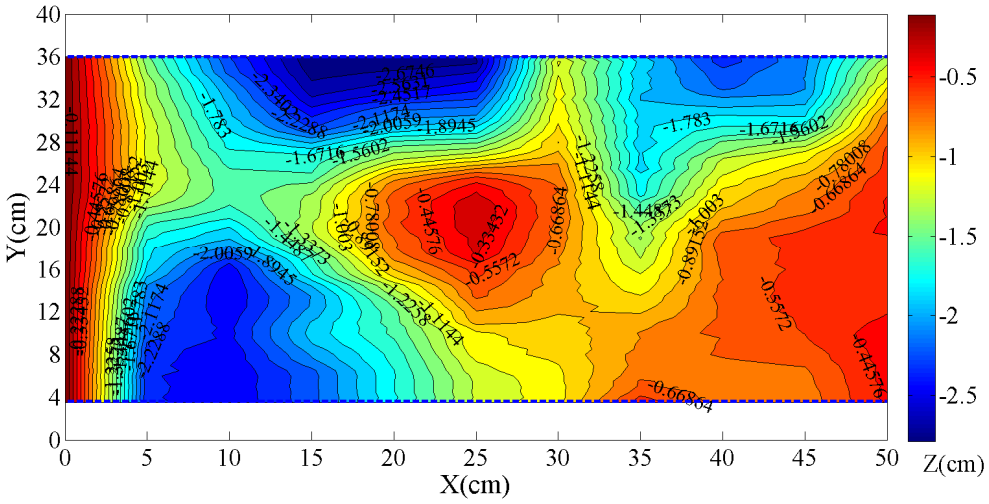

Figure 4.3 – Contour map of the analyzed channel reach.

In Figure 4.4 the instantaneous bed profiles measured in each investigated section are reported. The analysis of the instantaneous bed profiles confirms that during the process, near each bank a scour hole develops with a total length of about 30 cm. In particular, near the right bank the maximum scour depth is located at Y = 4 cm and between sections X10 and X15; the left bank the maximum scour depth occurs at Y = 36 cm and between sections X15 and X20. Between the lateral scour holes a central deposit takes places. The peak of this central deposit moves inside the region Y = 10 ÷ 20 cm. Approaching to section X30 the scour depths reduce. Downstream section X30 the scour depth increases only at the left bank and at the right bank a deposit occurs.

In order to better identify the geometric evolution of the scour holes observed in the considered channel reach (X0÷X50, see Figure 4.3), the longitudinal instantaneous bed profiles for different values of Y (with a mutual distance of 1 cm) are reported in Figure

4.5. The longitudinal bed profiles show that the maximum scour depth and the peak of the deposit do not maintain the same longitudinal position during the time. The longitudinal length and the depth of the scour hole modify in time. The trend of the instantaneous longitudinal profiles is similar for both the scour holes. Near the right bank, for Y < 15cm (see Figures 4.5a-c), the maximum scour depth moves between section X10 and X15, while near the left bank, for Y > 25 cm (see Figures 4.5e-g), the longitudinal position the scour depth of the maximum scour depth moves between sections X15 and X20. Moreover, near both banks the maximum scour depth moves along the vertical direction (with a vertical displacement of the maximum scour of about 1 cm). Approaching to the channel axis, for Y = 16÷24 cm the vertical displacement of the maximum scour increases. The longitudinal bed profiles (Figure 4.5) highlight that the maximum scour moves along the vertical and the longitudinal directions in time, but a sort of geometrical similarities can be observed. In order to analyze these similarities the normalized longitudinal profiles, for different values of Y (Y = 4÷36 cm), are reported in Figure 4.6. In this figure the longitudinal abscissa X is normalized by the total length L_{tot} (50 cm); the scour depth Z is normalized by the greatest value of the scour depth, Z_{min} (see the definition sketch of Figure 4.1). The reported longitudinal profiles has a mutual distance of dY = 3 cm. Figure 4.6 highlights the similarity of the measured bed longitudinal profiles. Moreover, it can be observed that the position of the maximum scour depth occurs for $0.3 < X/L_{tot} < 0.4$, in agreement with other experimental studies found in literature (Gaudio and Marion, 2003; Termini, 2007).

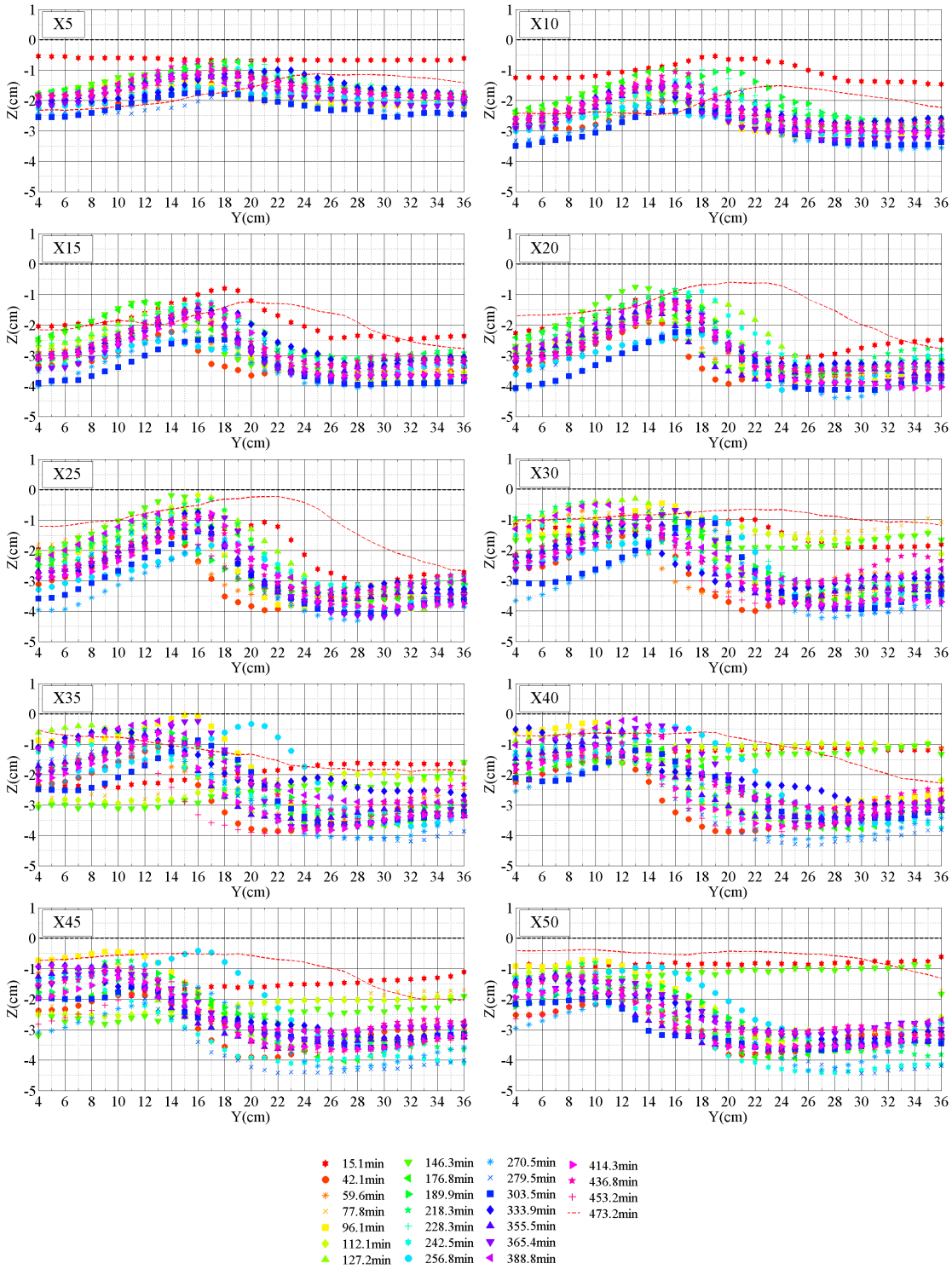

Figure 4.4 – Transversal instantaneous bed profiles.

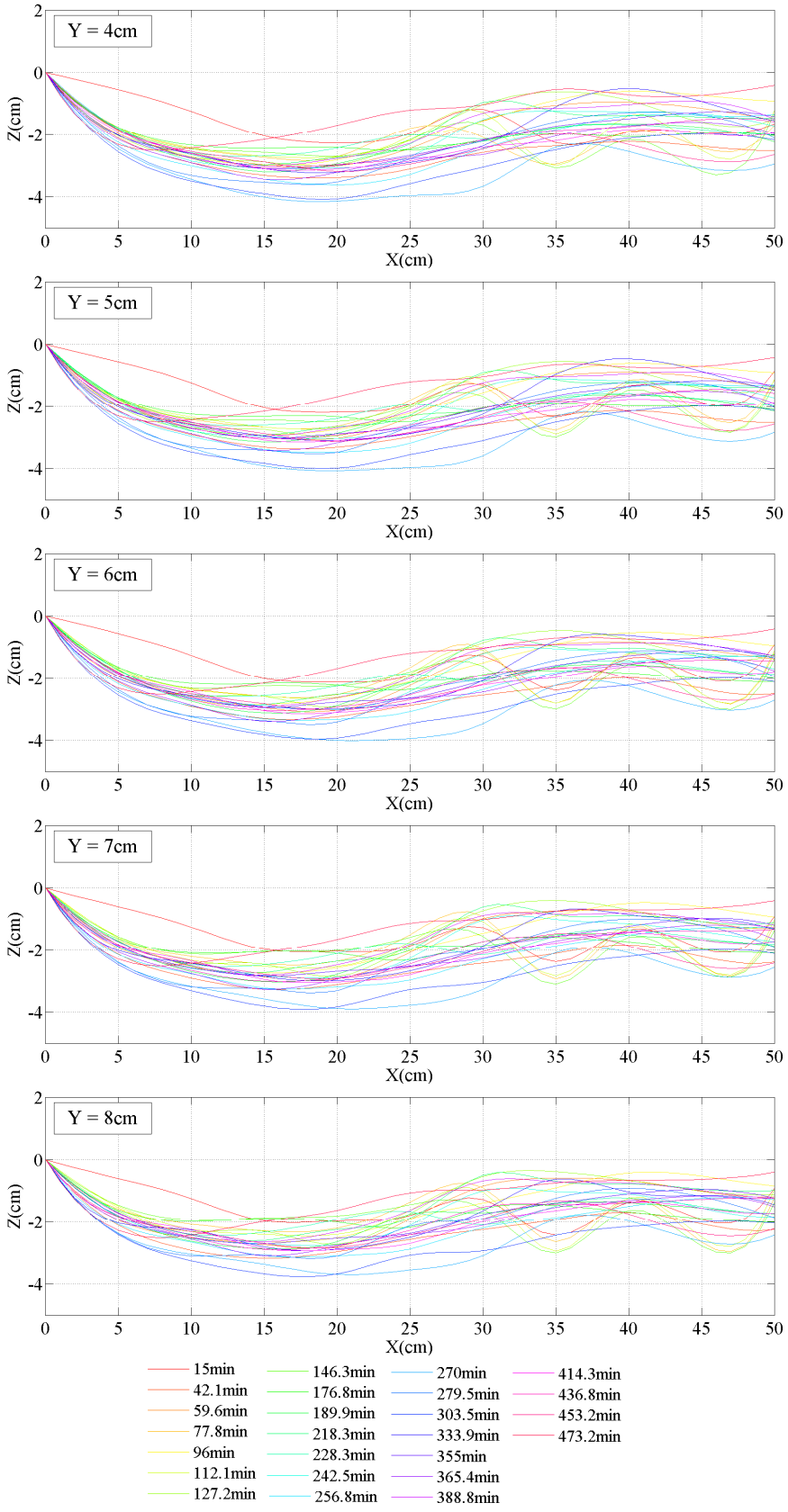

Figure 4.5 – Longitudinal instantaneous bed profiles: a) 4cm < Y < 8cm.

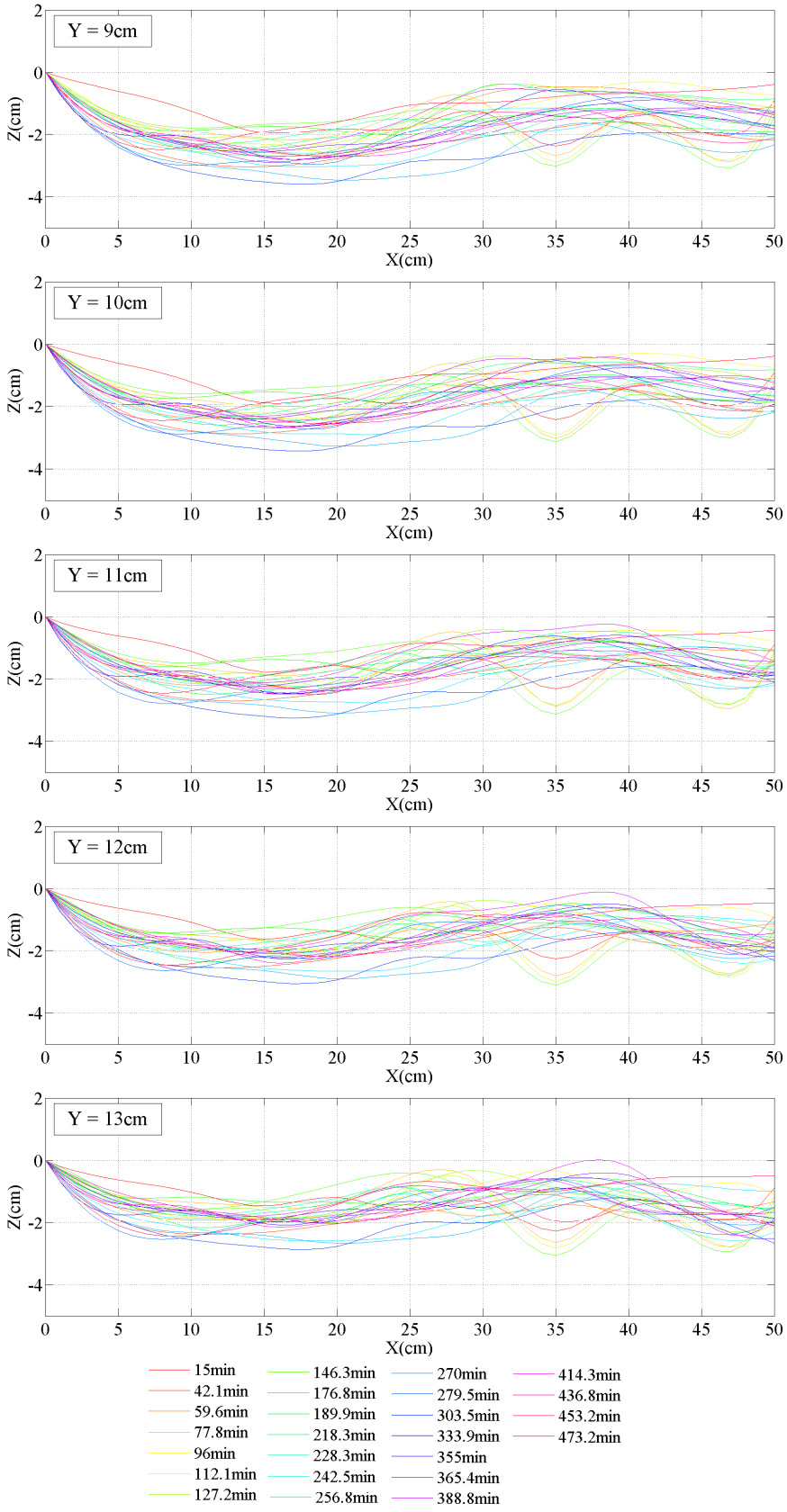

Figure 4.5 – Longitudinal instantaneous bed profiles: b) 9cm < Y < 13cm.

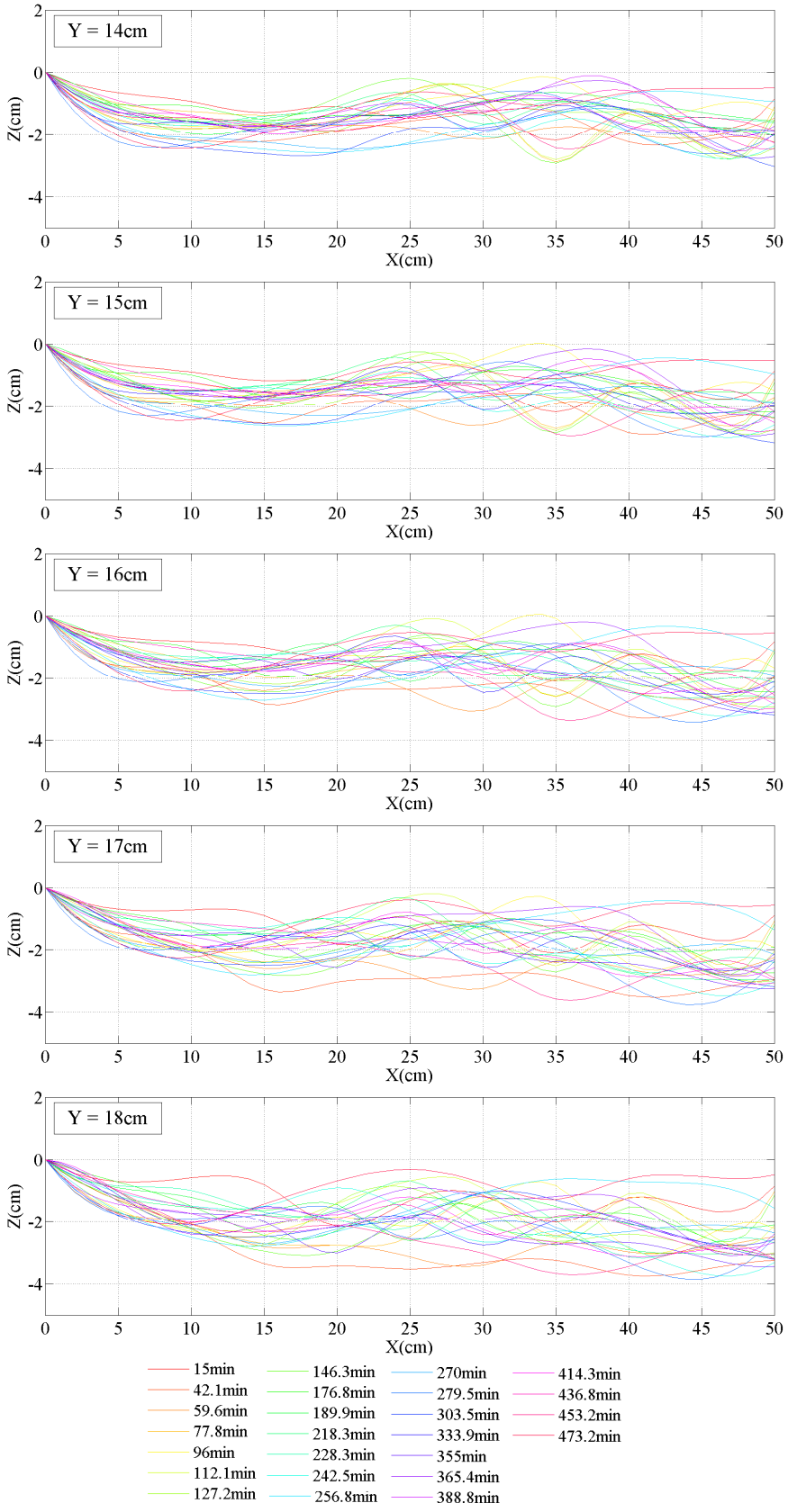

Figure 4.5 – Longitudinal instantaneous bed profiles: c) 14cm < Y < 18cm.

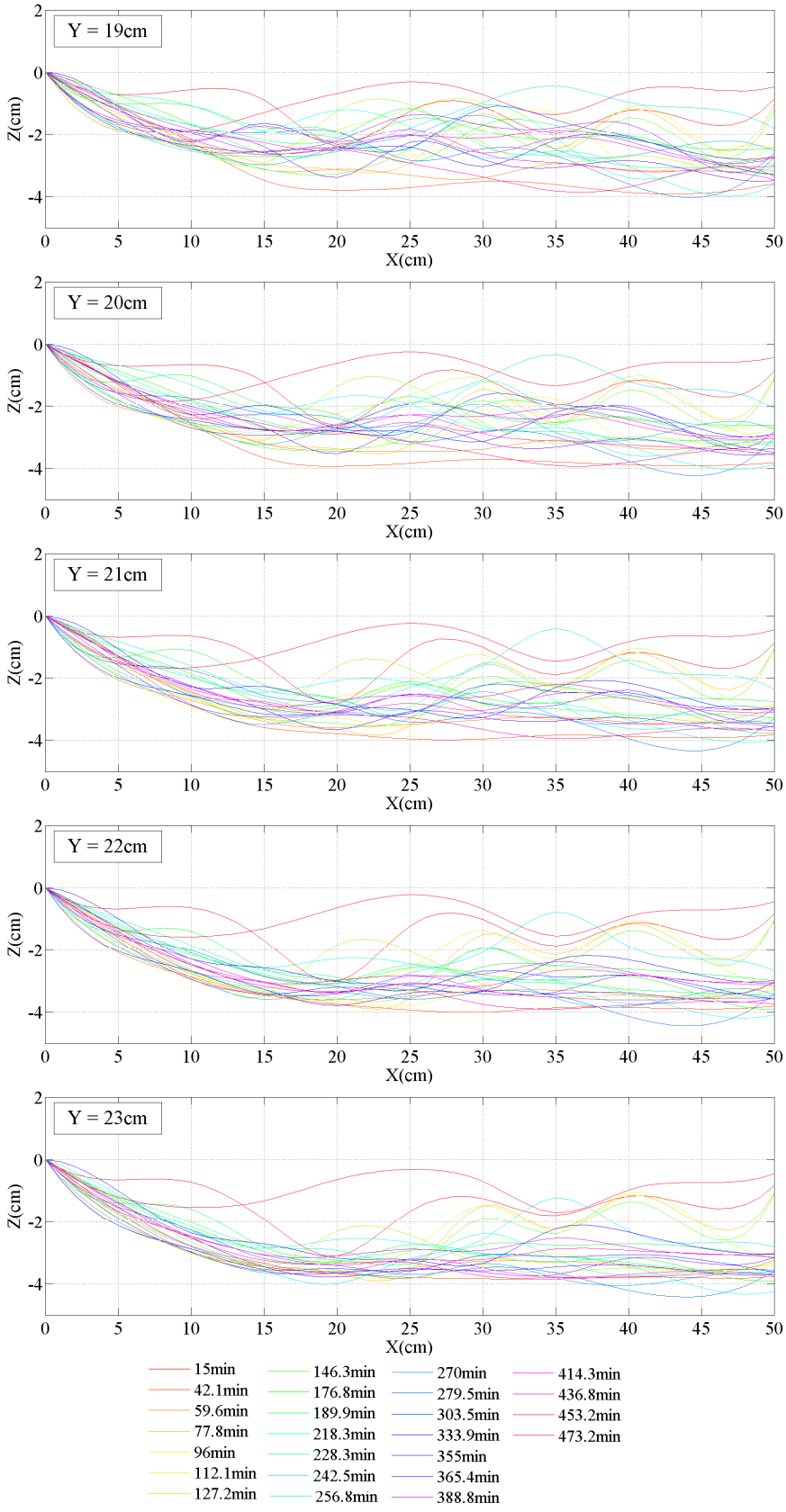

Figure 4.5 – Longitudinal instantaneous bed profiles: d) 19cm < Y < 23cm.

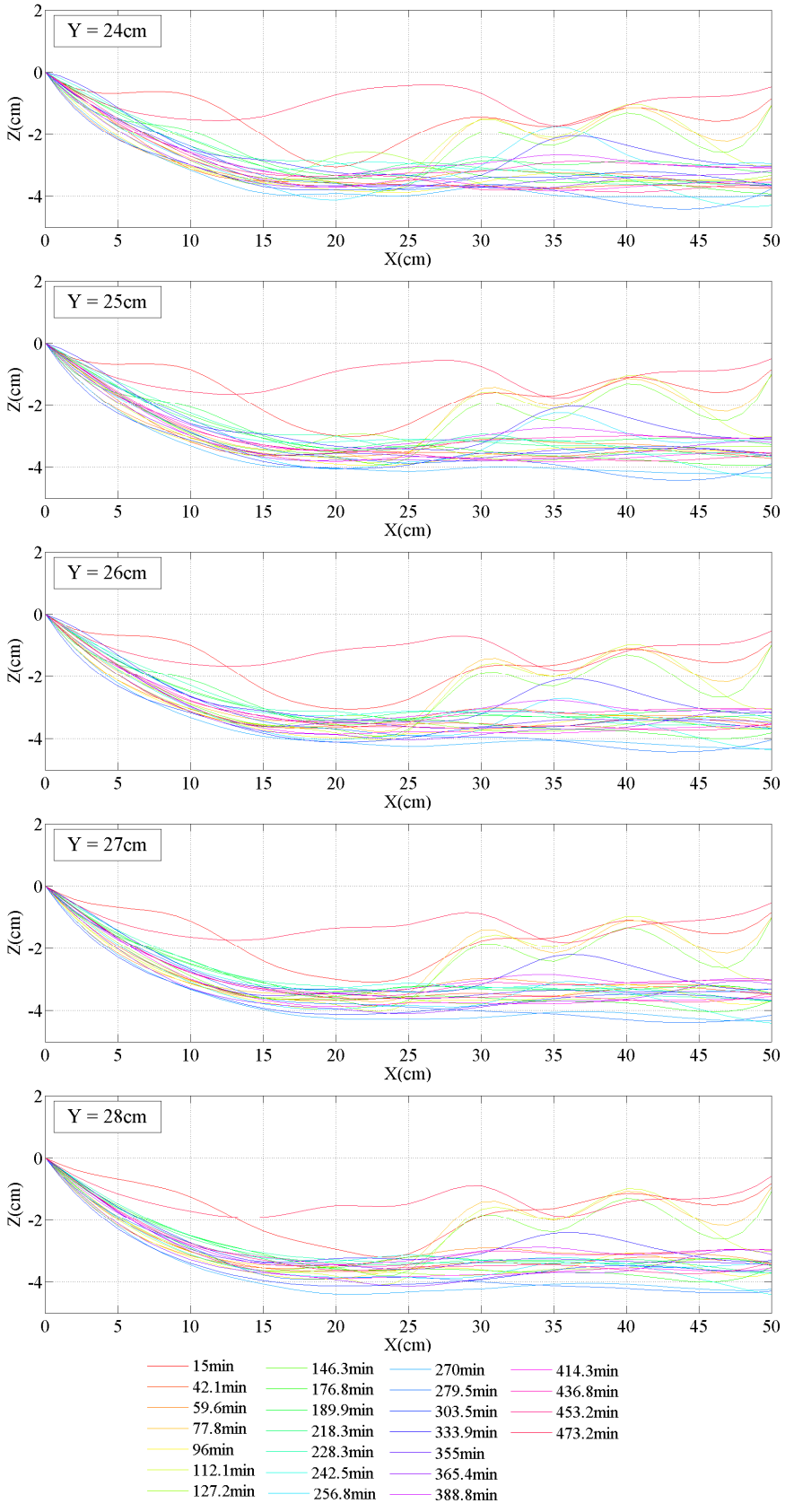

Figure 4.5 – Longitudinal instantaneous bed profiles: e) 24cm < Y < 28cm.

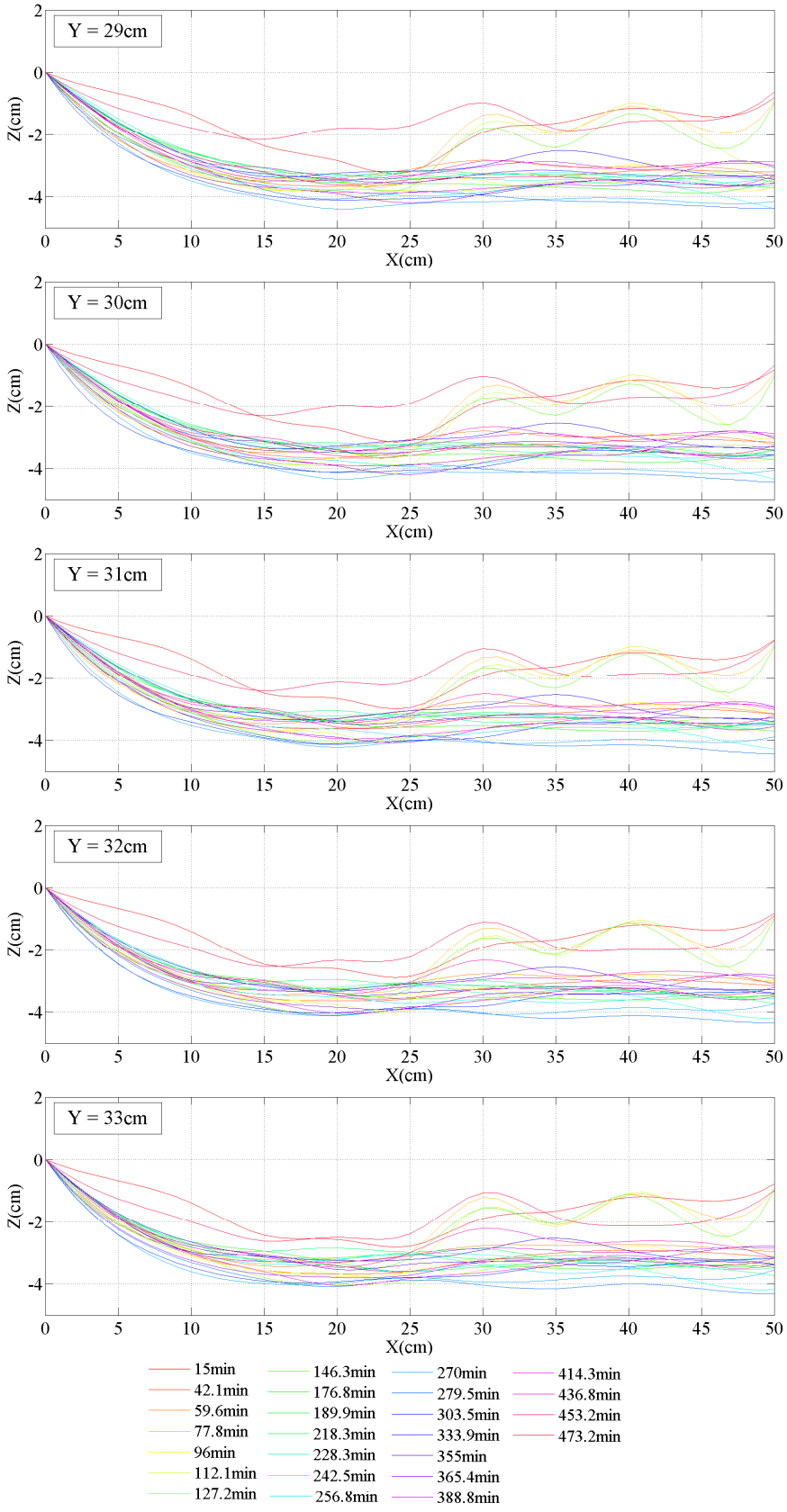

Figure 4.5 – Longitudinal instantaneous bed profiles: f) 29cm < Y < 33cm.

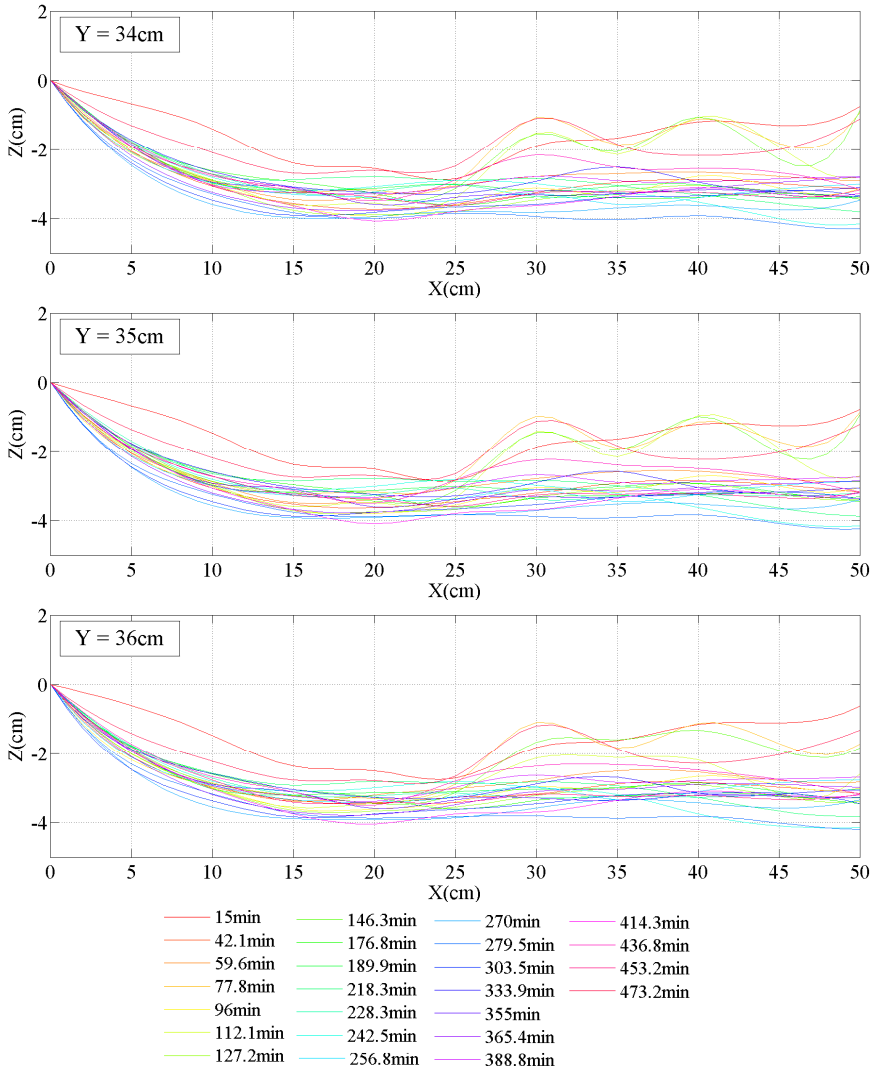

Figure 4.5 – Longitudinal instantaneous bed profiles: g) 34cm < Y < 36cm.

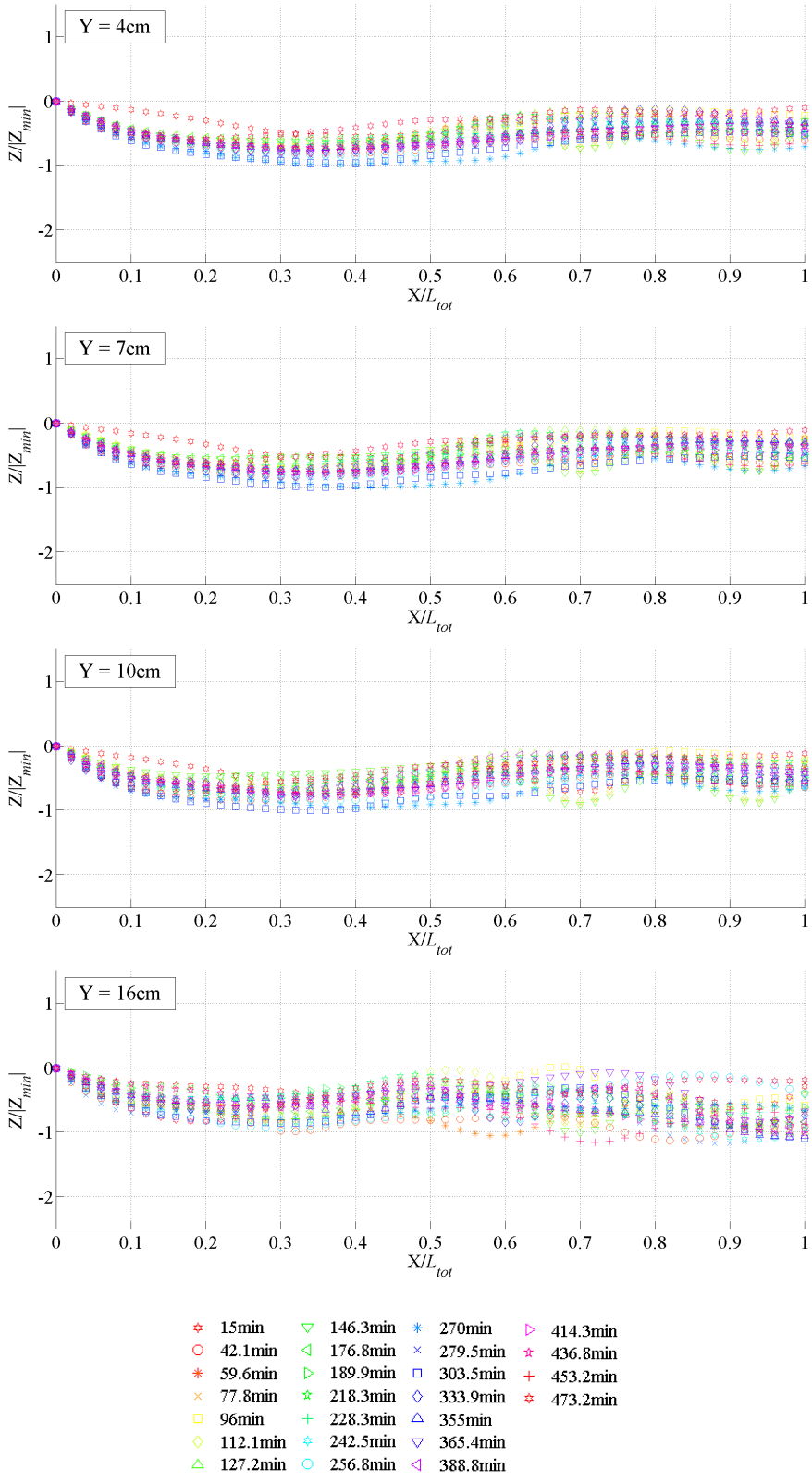

Figure 4.6 – Normalized longitudinal profiles: a) 4cm < Y < 16cm.

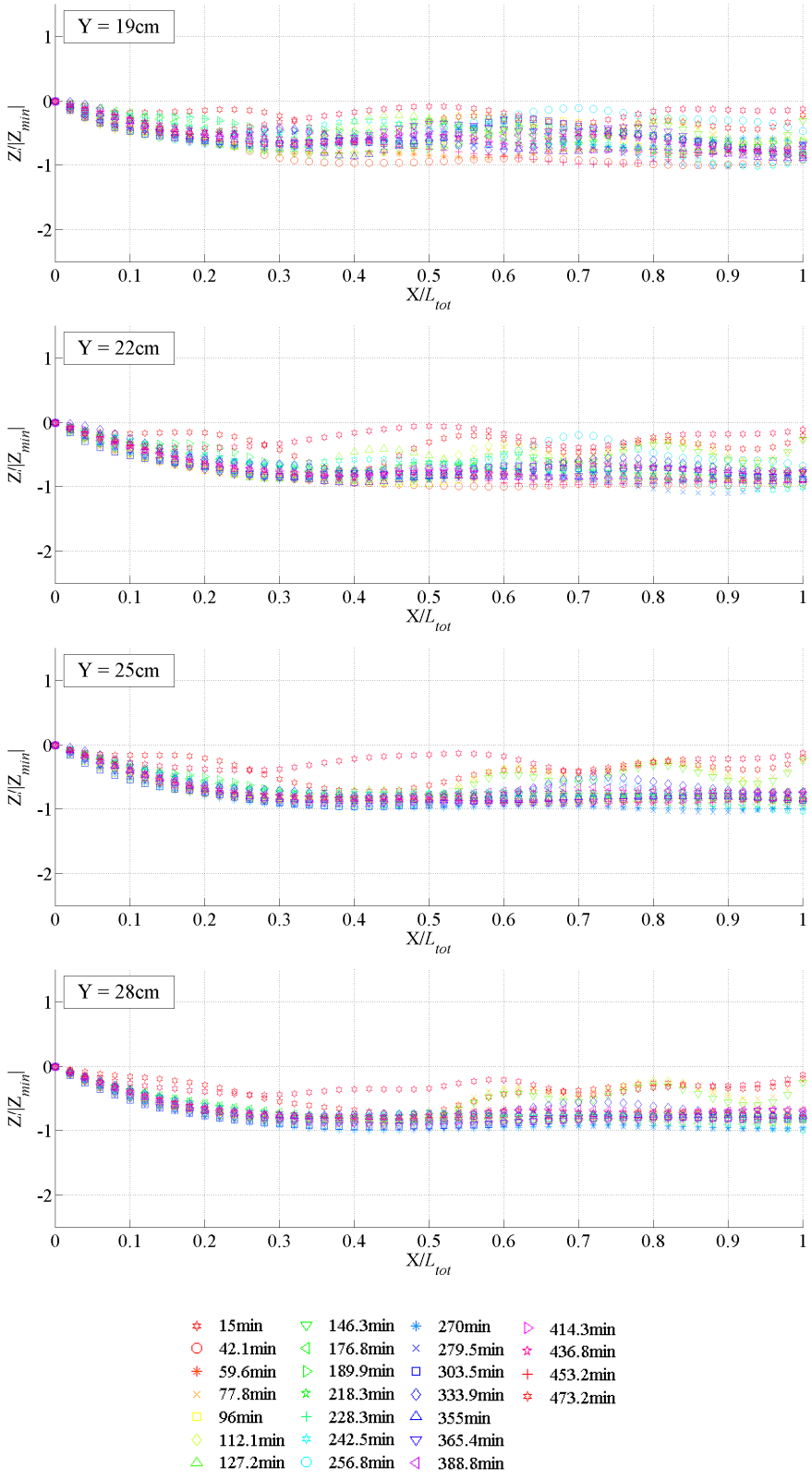

Figure 4.6 – Normalized longitudinal profiles: b) 19cm < Y < 28cm.

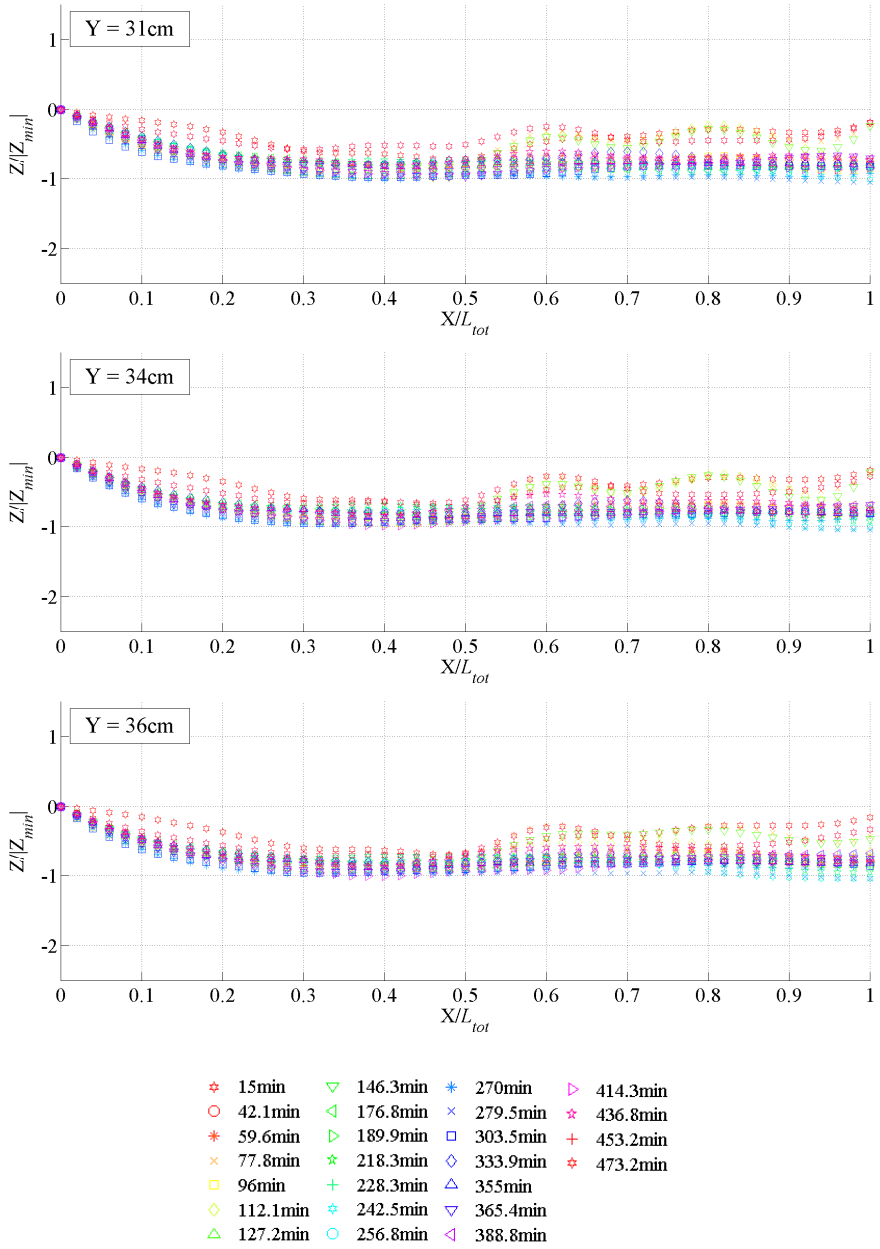

Figure 4.6 – Normalized longitudinal profiles: c) 31cm < Y < 36cm.

In order to better understand the temporal evolution of the scour position, the geometrical characteristics of the scour hole have been analyzed for the considered measurement points within the analyzed channel reach (X0÷X50). For each longitudinal instantaneous bed profiles (Y = 4 ÷ 36 cm with a step dY = 3 cm) the geometric parameters of the scour hole (see the definition sketch of Figure 4.1) have been considered at each time *t*: the greatest value, in modulus, of the scour depth at time *t*, $Z_{min,t}$; the

maximum scour depth occurring of excavation at the transversal abscissa Y, Z_{min}; the instantaneous longitudinal distance of the maximum scour L_{max} from the first section X0; the instantaneous longitudinal distance L_t of the deposit crest occurring downstream of the scour hole. The temporal evolution of these parameters allow us to analyze the vertical and horizontal time development of the scour hole.

The time evolution of the maximum scour depth $|Z_{min,t}|$ and of the no-dimensional maximum scour depth $Z_{min,t}/Z_{min}$ (for each transversal abscissa Y) are reported, in Figure 4.7 and in Figure 4.8 respectively. In these figures the time t has been normalized by the total observation time T = 480 min. From these figures it can be observed that for Y≤ 13cm, the temporal evolution of $|Z_{min,t}|$ and of $Z_{min,t}/Z_{min}$ is characterized by four phases. For each value of the considered abscissa Y, the maximum scour depth develops very quickly during the first minutes (t/T < 0.1) and becomes slower and slower through the time. At t/T = 0.1 the scour depth assumes a peak value: near the right bank for Y = 4 ÷ 13 cm it is $Z_{min,t}/Z_{min}$= 0.8; near the channel axis, for Y = 16 ÷ 22 cm, it is $Z_{min,t}/Z_{min}$= 1; near the left bank, for Y = 25 ÷ 36cm, it is $Z_{min,t}/Z_{min}$= 0.9. In a second phase (0.1 < t/T <0.4) the time gradient of the scour depth gradually decreases, maintaining a constant value lower of about 10÷20% of the first peak (for Y < 25 cm). Close to the left bank, for Y ≥ 25 cm, the plots show that after the first peak the scour depth almost assumes a constant value ($Z_{min,t}/Z_{min}$≅ 0.9). In the third phase (0.4 < t/T < 0.6) the local vertical erosion increases again until that (0.6 < t/T < 1) it slightly decreases, reaching an almost constant value. In the four phase the maximum scour depth $Z_{min,t}$ fluctuates around a mean "equilibrium" value of $Z_{min,t}/Z_{min}$ ≅ 0.8. Thus, in agreement with other experimental literature studies (Richardson and Davis, 2001), the fluctuations of the maximum scour depth $Z_{min,t}$ are about 10% either side of the equilibrium value.

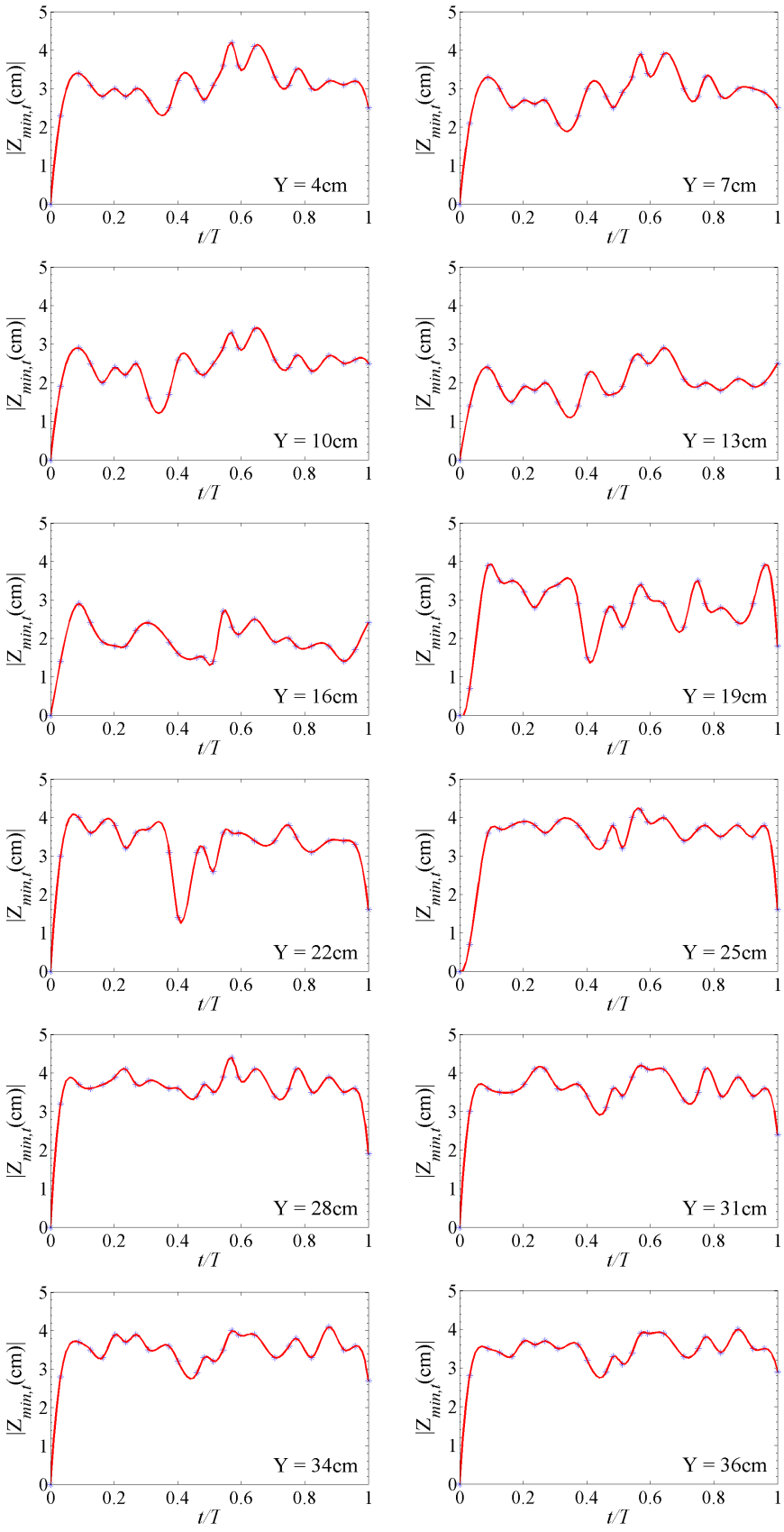

Figure 4.7 - Time evolution of the absolute value of maximum scour depth $Z_{min,t}$.

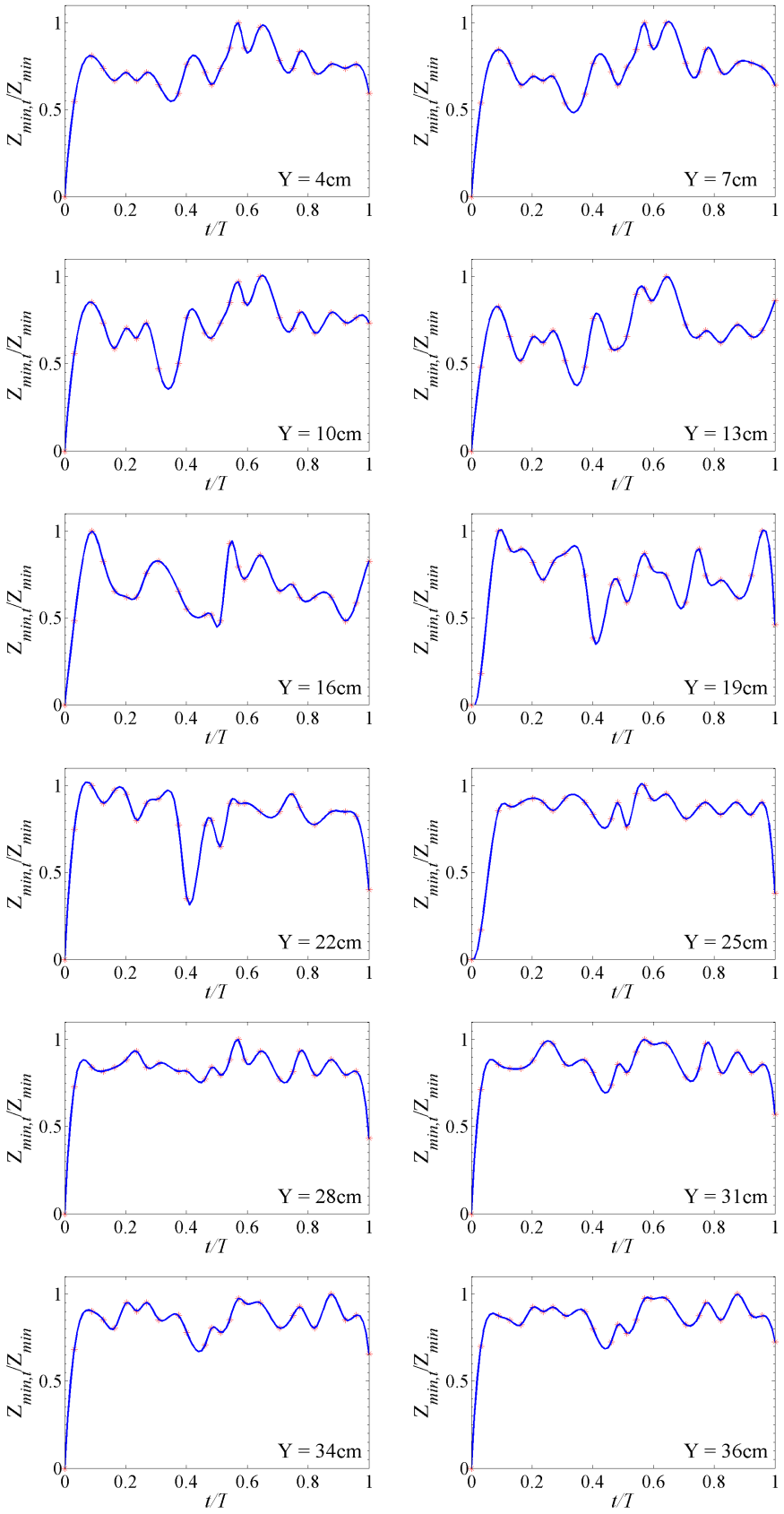

Figure 4.8 - Time evolution of the no-dimensional maximum scour depth $Z_{min,t}/Z_{min}$.

In order to analyze the time development of the scour hole along the longitudinal direction, the time evolution of L_{max} and L_t versus the normalized time t/T, for the considered values of Y, have been reported in Figure 4.9 and in Figure.10. In these figures L_{max} and L_t have been normalized by the total length of the scour phenomenon L_{tot}. These figures show that the temporal evolution of the scour process, along the longitudinal direction, is characterized by two phases. In the first phase, t/T < 0.1, L_{max} and L_t increase quickly; in the second phase, t/T > 0.1, each variable fluctuates around a mean value that change with the transversal abscissa Y. In particular, L_{max} fluctuates about the 30% of the total length L_{tot} ($L_{max} / L_{tot} \cong 0.3$), from the right bank to the channel axis (4 cm < Y < 19 cm). Thus the maximum scour depth is localized at section X15. Approaching to the left bank, for Y > 22 cm, is $L_{max} / L_{tot} \cong 0.4$, so that the maximum scour depth moves from section X15 to section X20. The crest of the sand deposit does not change position during the scouring development maintaining a distance from section X0 of about 30 cm. In fact, the time-average value of L_t / L_{tot} is about 50÷60%. Thus, the erosion develops more in vertical direction than in longitudinal.

On the basis of the aforementioned analysis it has been observed that the bed profiles and of the geometric parameters of the scour hole vary along three directions.

In order to understand how erosion process is distribuited along the interested zone, by using the instantaneous DEM of the bed, the eroded sand volume, for each section Xj, W_X, and for each transversal abscissa Y, W_Y, has been estimated.

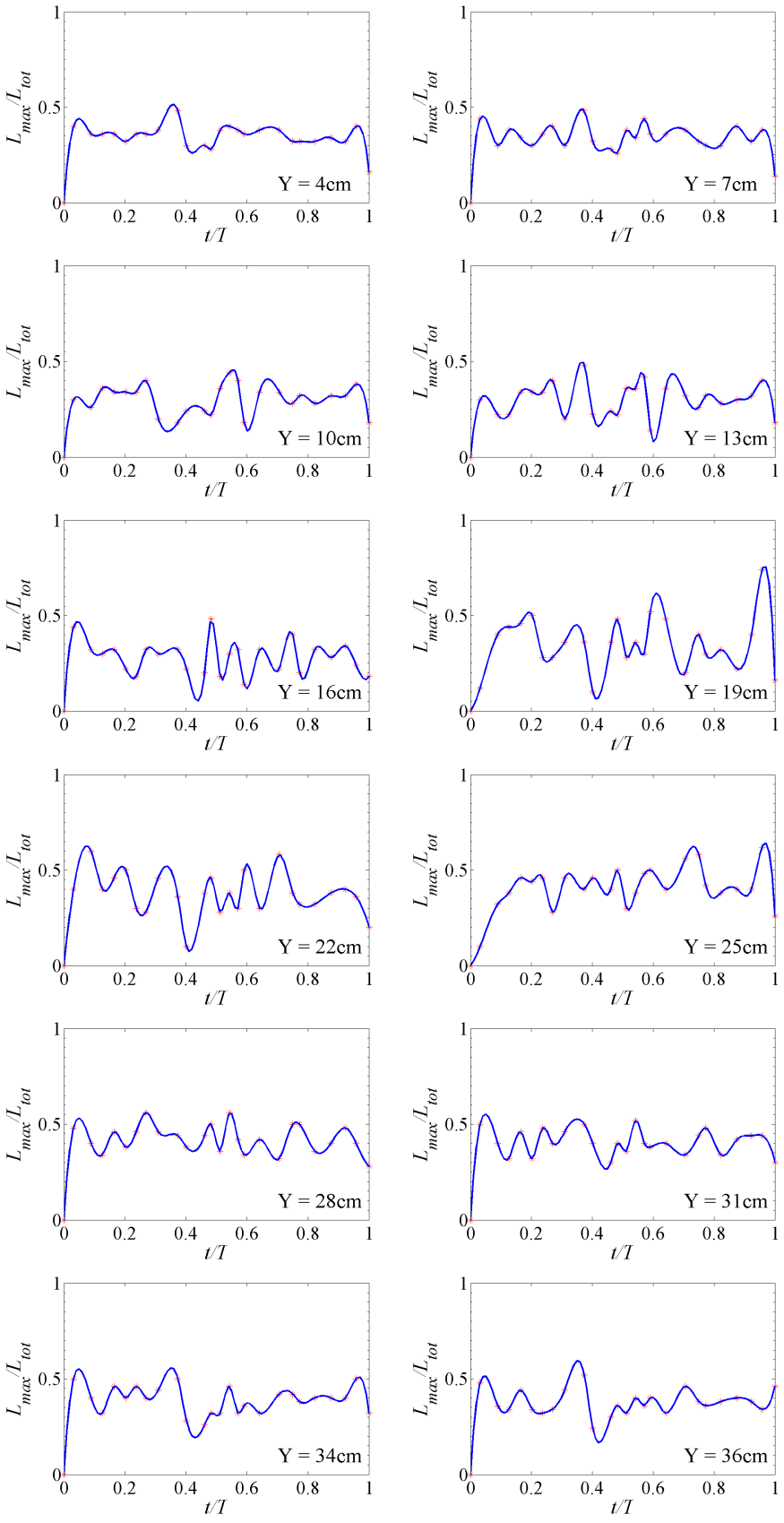

Figure 4.9 - Time evolution of the no-dimensional horizontal distance of the maximum scour L_{max}/L_{tot}.

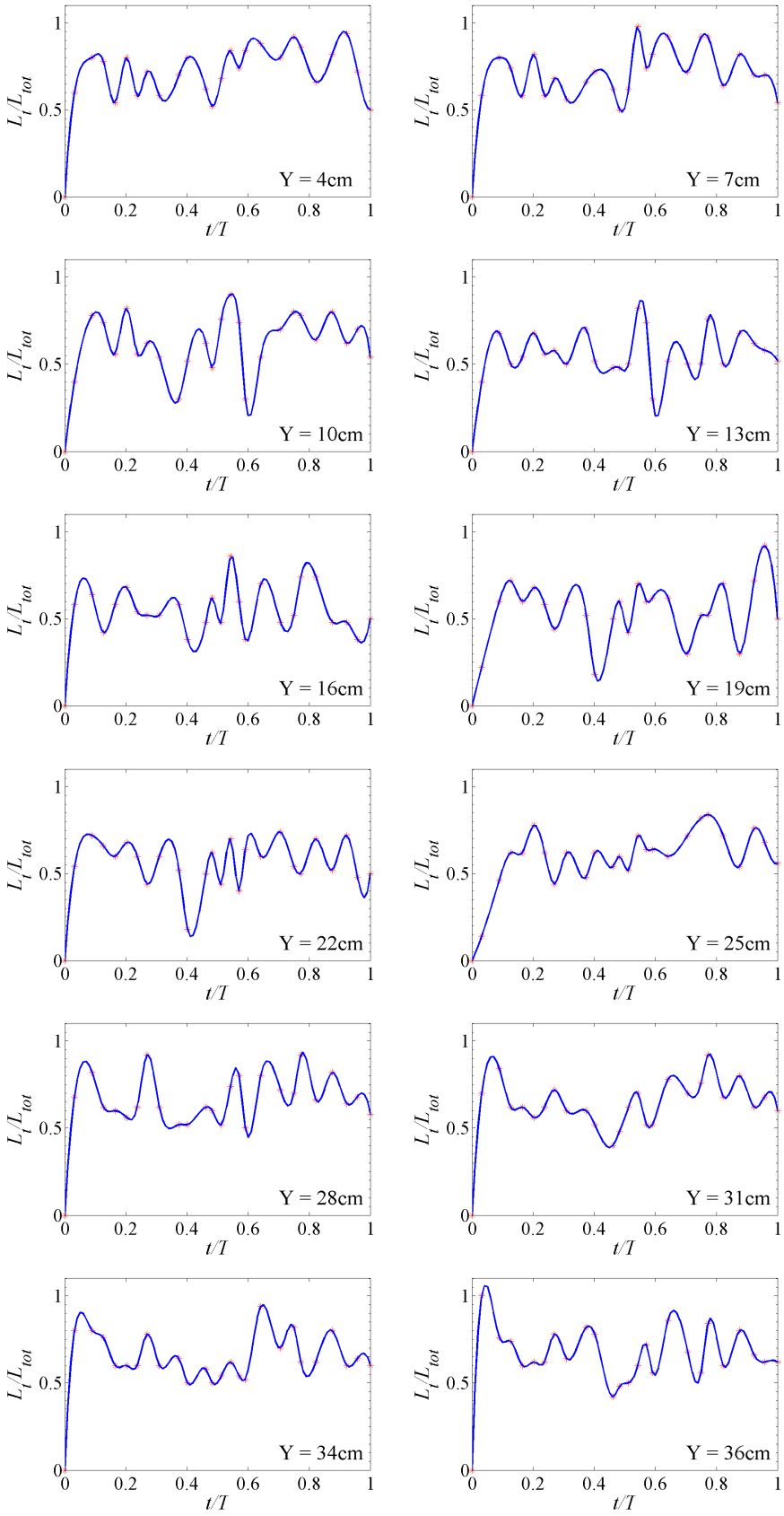

Figure 4.10 - Time evolution of the no-dimensional horizontal scour length L_t/L_{tot}.

Thus, the bed cross section has been divided into four equal parts and for each of them the erosion volume has been computed (see Figure 4.11). For each cross section the relative erosion volume has been computed as the sum of the four erosion volumes $W_{X,i}$ (i-*th* portion of the eroded bed, i = I,…,IV):

$$W_X = W_{X,I} + W_{X,II} + W_{X,III} + W_{X,IV} \quad (4.1)$$

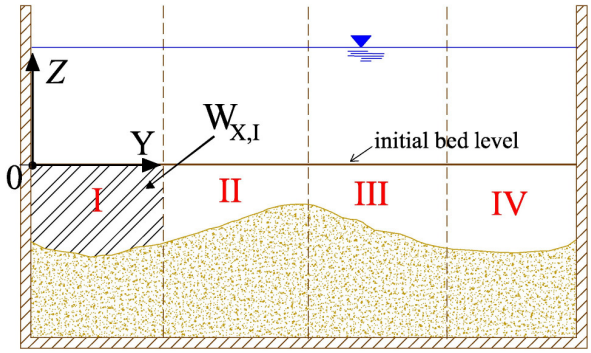

Figure 4.11 – Scheme to compute the eroded volume .

Thus, for each cross section Xj the transversal eroded volumes W_X, $W_{X,I}$ $W_{X,II}$ $W_{X,III}$ and $W_{X,IV}$ have been calculated for each instant *t* and these volumes are plotted in Figure 4.12. In these figure the eroded volumes per unit length are plotted versus the no-dimensional time *t*/T. The analysis of the time evolution of the eroded volumes confirms that the scouring process develops into four phases. During the early minutes of the scouring process, t/T <0.1, W_T increases quickly reaching a peak value at *t*/T = 0.1. The peak value of W_T increases moving towards section X20 ($W_T \cong 100$ cm^3/cm) and decreases towards section X25 ($W_T \cong 85$ cm^3/cm). For *t*/T = 0.2 ÷ 0.4 the eroded volume reduces its gradient and maintains a constant value. In a third phase (0.4 < *t*/T < 0.6) the erosion volume increases again until that, for *t*/T > 0.6, W_T fluctuates around a mean "equilibrium" value.

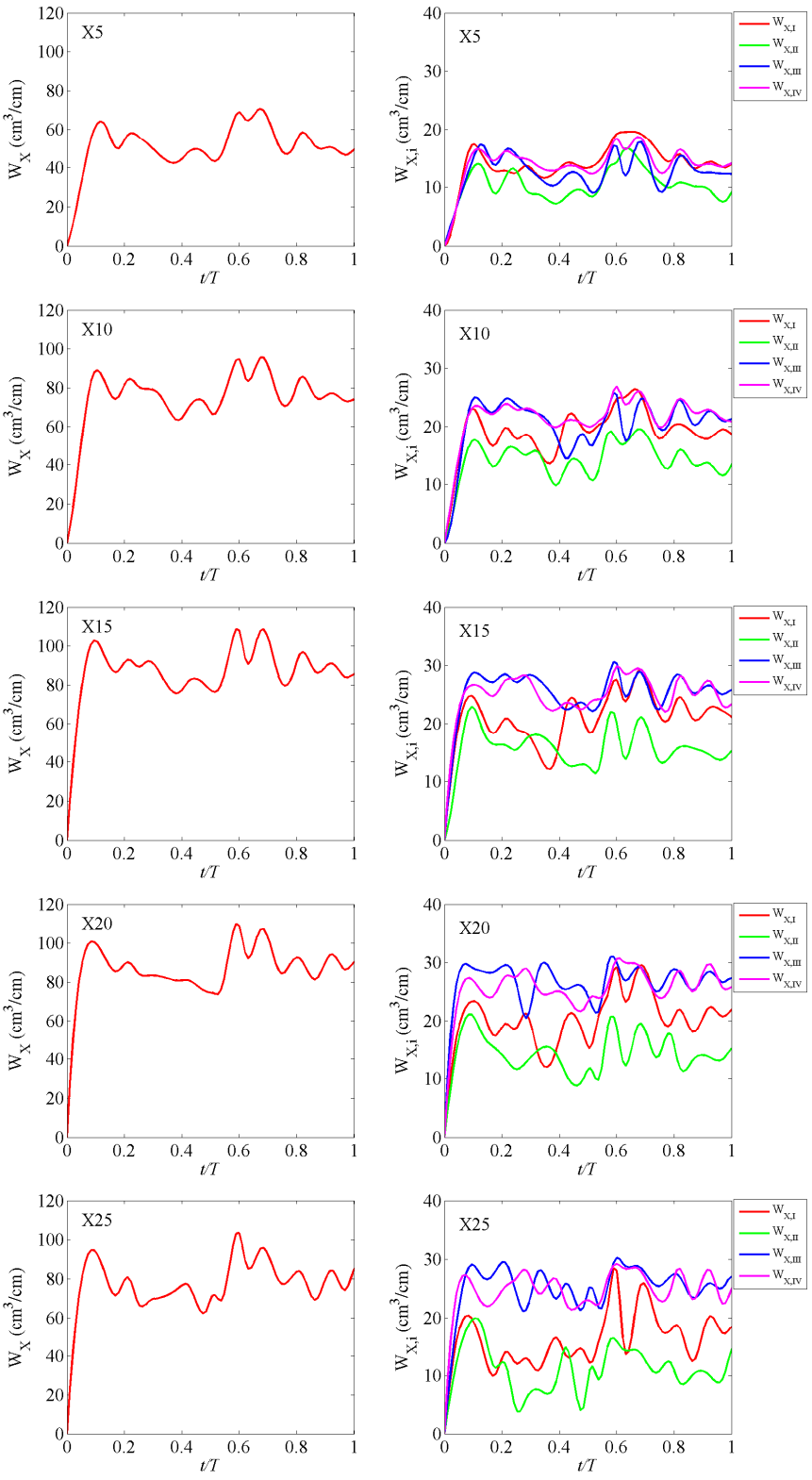

Figure 4.12 – Time evolution of the eroded volumes W_X and $W_{X,i}$: a) sections X5÷X25.

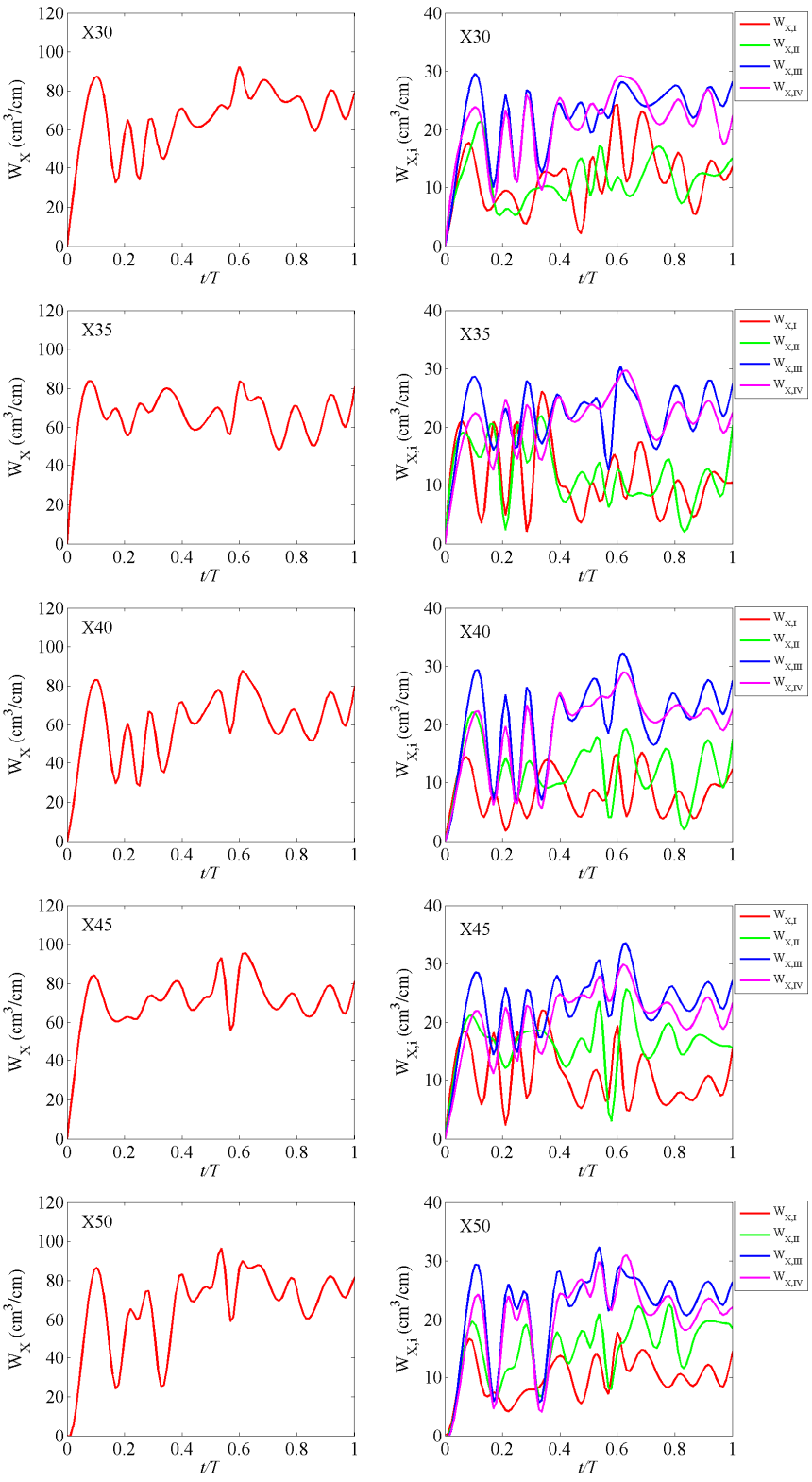

Figure 4.12 – Time evolution of the eroded volumes W_X and $W_{X,i}$: b) sections X30÷X50.

The equilibrium value of the volume eroded seems to be greater at section X20.For section downstream of X25 (see plots in Figure 4.12b) the trend of the eroded volume W_X is still characterized by four phases, but, in this case, the plots present strong oscillations after the second phase, for $t/T > 0.1$. For $t/T > 0.4$ the eroded volume begins to increase with high fluctuation around the equilibrium value. For X<X15 (see Figure 4.12a) the scouring contribution of the left part (Y > 20cm) is greater than that of the right part, in fact the values of $W_{T,III}$ and $W_{T,IV}$ are greater than $W_{T,I}$ and $W_{T,II}$ during time. Moving towards section X30, the contribution of the left scour begins predominant over the right scour. For section downstream of X30 (downstream of the deposit) during the second phase of the scouring process, for $t/T < 0.4$, the trend of the volumes $W_{T,III}$ and $W_{T,IV}$ is characterized by high oscillations; the curves of $W_{T,III}$ and $W_{T,IV}$ cross those $W_{T,I}$ and $W_{T,II}$. Finally, in Figure 4.13, for each considered transversal abscissa Y (with a step of dY = 3 cm) the eroded volumes W_Y, per unit width, have been plotted versus the no-dimensional time t/T. The trend of W_Y confirms the trend previously observed. In general, the temporal evolution of W_Y is defined by four phases. Near the right bank, Y < 16cm, during the final phase ($t/T > 0.6$) the mean value of the eroded volume W_Y is about 250 cm^3/cm and approaching towards the channel axis it decreases assuming, at Y = 16 cm, a final mean value $W_Y = 100 cm^3/cm$.

Moving toward the left bank (Y = 36 cm) the final phase has a mean value greater than that observed at the channel axis, $W_Y = 250$ cm^3/cm. Thus, at the channel axis the rate of erosion seems to be lower than that observed near bank regions, where similar values of eroded volume have been detected ($W_Y \cong 250 cm^3/cm$).

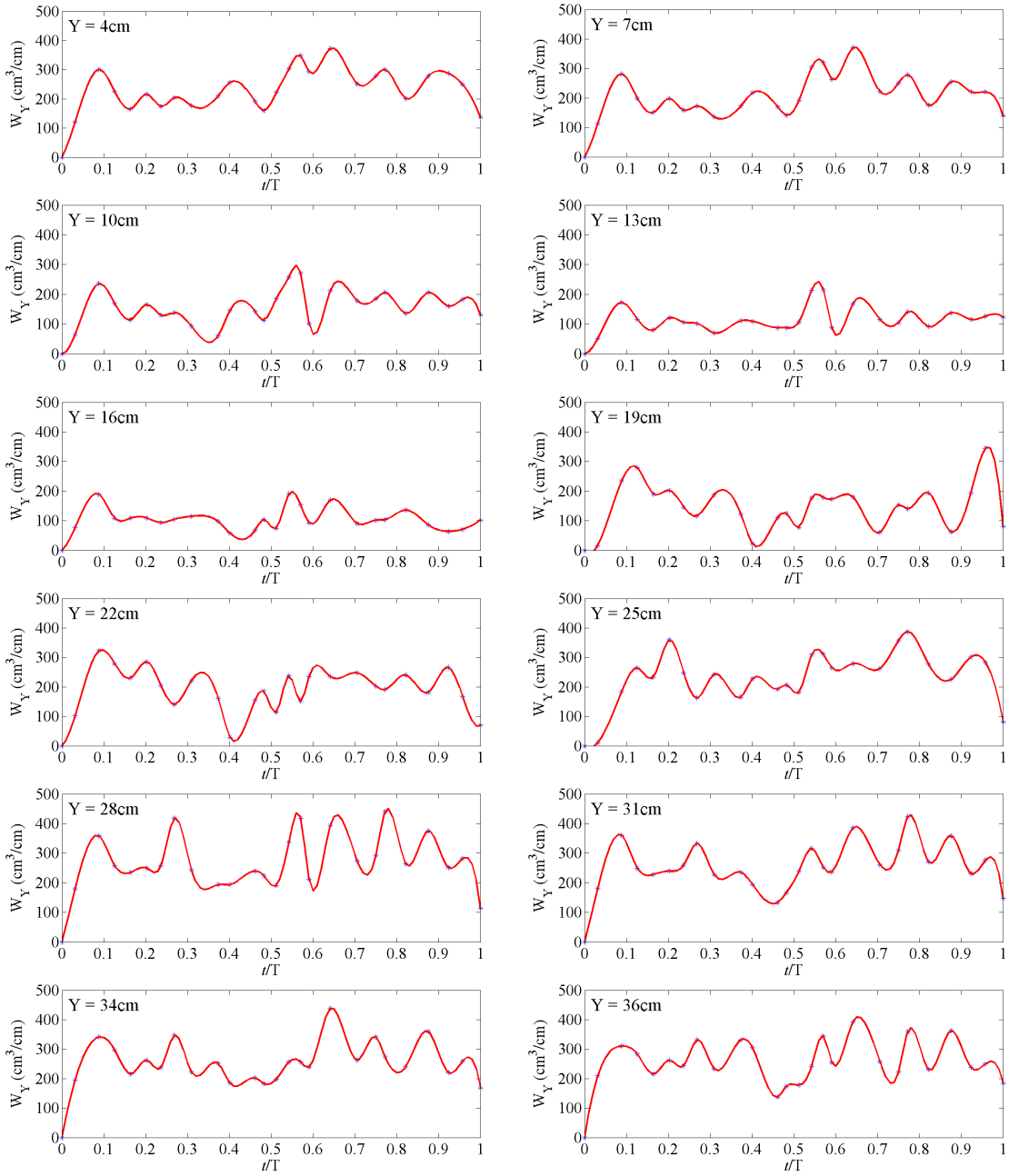

Figure 4.13 – Time evolution of the eroded volumes W_Y.

The analyses of the transversal and longitudinal eroded volumes has highlighted that the contribution of the left bank is similar to that of the right bank during the scouring process. Two scour holes have been observed. Each of them develops with the same trend: the maximum scour depth Z_{min} obtained at the "equilibrium" phase is similar for both the scour holes assuming a value of 3.5 cm for Y = 4 cm and Y = 36 cm; the maximum

longitudinal distance of the deposit crest L_t assumes a value of 30 cm. Thus, near each bank the scour hole assumes a length of 30cm at the equilibrium. Downstream of each scour holes small sand deposit take place. Between the scour holes, in the transversal direction the bed reduces its depth, in fact the rate erosion of this region (15cm < Y < 25cm) is lower than the other (see Figure 4.13).

In order to better understand how these scour holes develops during the scouring phenomenon, the temporal evolution of the geometric parameters shown in Figure 4.14 has been analyzed.

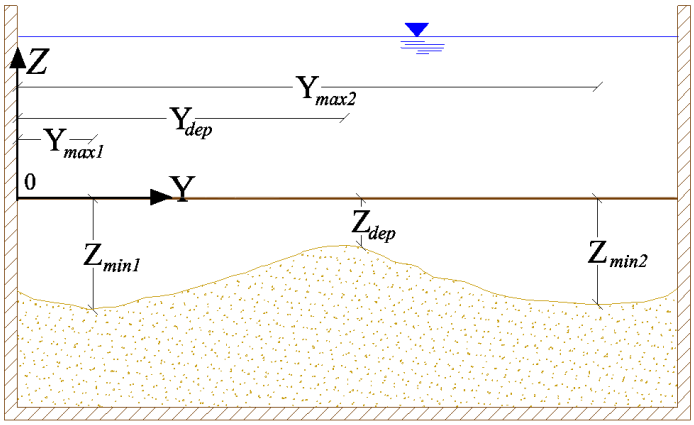

Figure 4.14 - Definition sketch of the geometric parameters: Z_{min1}, Z_{min2}, Y_{max1} , Y_{max2} , Y_{dep} and Z_{dep}.

These parameters have been adimensionalized with respect to the channel width (B = 0.4 m). The temporal variations of these adimensionalized parameters are represented in Figure 4.15. As shown in this figure, almost in every cross sections, the two scours hole and the deposit are identifiable. Two zones can be indentify: a first zone, for X0 < X < X30, and a second zone, for X30 < X < X50. For the first zone, the deposit crest occurs at about an half of the channel (Y_{dep}/B ≅ 0.4), the maximum scour near the right bank maintains a constant distance from the bank (Y_{max1}/B ≅ 0.1), while the maximum of the

scour near the left bank takes a variable position during all the process ($0.5 < Y_{max2}/B < 0.8$). In particular, at the beginning the scour near the left bank it seems to occur at the channel axis ($Y_{max2}/B \cong 0.5$), then, during the process, it moves away from the axis, getting closer to the left bank ($Y_{max2}/B \cong 0.8$). This variation is more evident in sections X5 and X20. For the remaining sections of the first zone ($Xj \leq X30$), the trend is similar, but the scour near the left bank starts close to the channel axis, then it moves away from the channel axis reaching positions closer and closer to the left bank ($Y_{max2}/B \cong 0.8$). In the second region, during all the process, the deepest scour is near the right bank and it maintains a constant distance from the right bank ($Y_{max1}/B \cong 0.1$); the highest point of the deposit, after about 170 minutes ($t/T > 0.4$), remains close to the right bank ($Y_{max1}/B \cong 0.2$). Furthermore it is possible to observe that for the deepest scour near the left bank some temporal "gap" occurs, i.e. the curves present points of discontinuity. These discontinuities indicate that in the analyzed section at some instants a deeper point ($Y_{max1}/B \cong 0.1$) occurs. This phenomenon occurs for $t/T < 0.3$. This trend is definitely more evident for sections X40 and X45. From this analysis, it is possible to conclude that in the first zone ($X < X30$) the presence of two scour remains steady in time, but in the second zone two different time phases separated by the instant $t/T=0.4$ are observed. During the first phase, alternating movements of the deposit from the left to the right occur. In figure 4.16, the trends of Z_{min1} and Z_{min2} are shown for each cross section. These plots highlight that section X5 the temporal profiles of maximum scours (Z_{min1} and Z_{min2}) are practically coincident. The trend is characterized by a rapid increase of the maximum value during the first $t/T < 0.1$, then the maximum scour maintains almost constant value until $t/T = 0.4$. Then a further increase of the maximum scour occurs until to reach a constant value ($t/T > 0.6$). Evident oscillations can be observed starting from the section X30. In these sections two points of discontinuity appear.

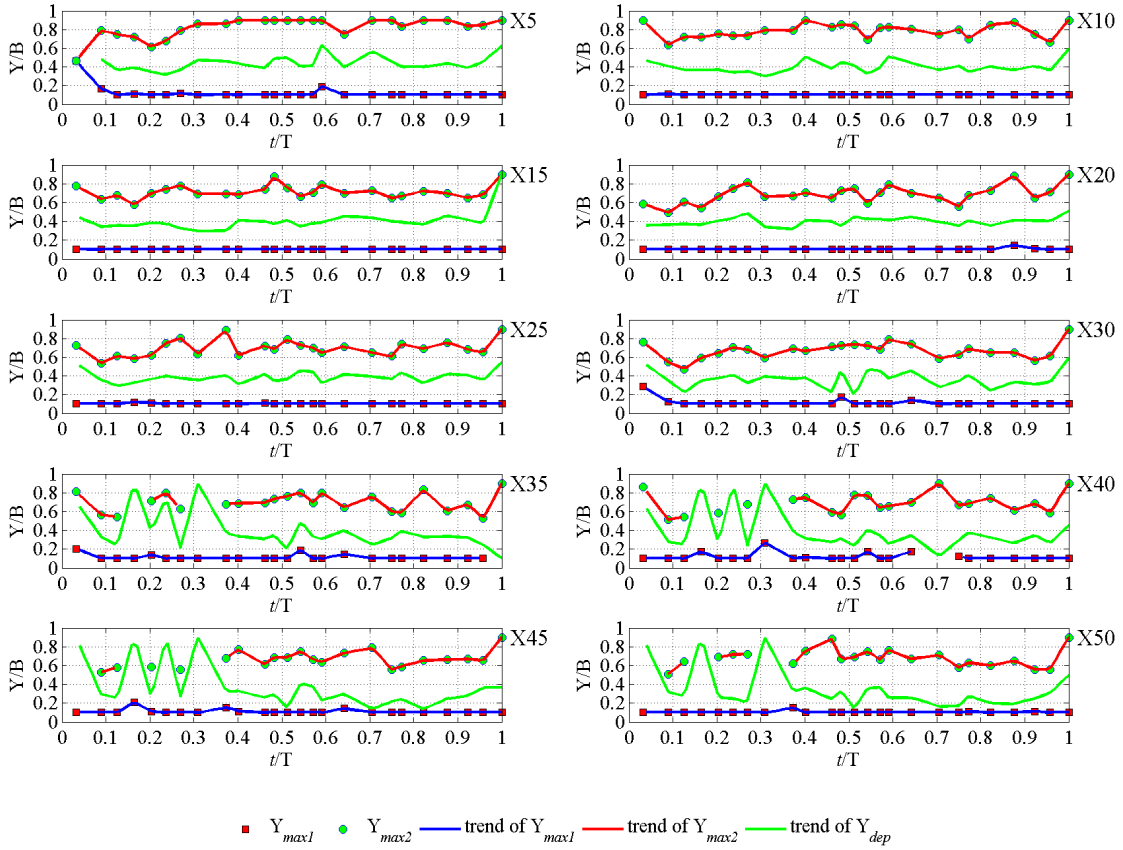

Figure 4.15 – Time development of $Y_{max,1}$, $Y_{max,2}$ and Y_{dep}.

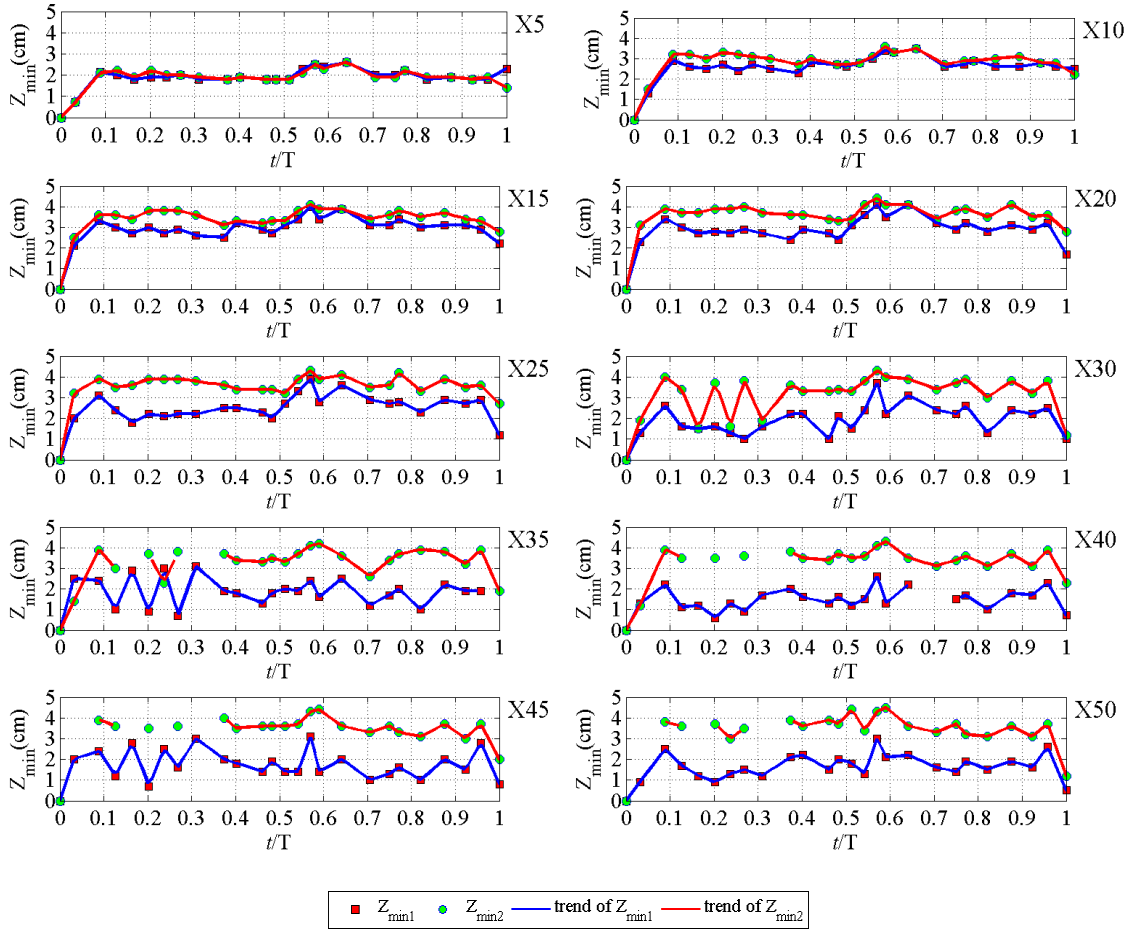

Figure 4.16 – Time development of $Z_{min,1}$ and $Z_{min,2}$.